CONTRIBUTIONS
to SCIENCE
OPEN ACCESS

# The contribution of the Barcelona World Race to improved ocean surface information. A validation of the SMOS remotely sensed salinity

**Jordi Salat, Marta Umbert, Joaquim Ballabrera-Poy, Pedro Fernández, Kintxo Salvador, Justino Martínez**

Institute of Marine Sciences (ICM-CSIC), Barcelona, Catalonia

**Correspondence:**
Jordi Salat
Institut de Ciències del Mar (ICM-CSIC)
Pg. Marítim de la Barceloneta, 37-49
08003 Barcelona, Catalonia
Tel.  +34-932309511
Fax  +34-932309555

**Summary.** The oceans not only cover about three quarters of the Earth's surface but they also constitute the most relevant climate driver. However, our present knowledge about the oceans is by no means comparable to that of terrestrial or atmospheric systems. Salinity and temperature are key parameters to understand the dynamics of the oceans; but a global network of observations is lacking in spite of valuable data on the oceans that are being accumulated through oceanographic campaigns and by using automated devices, fixed moorings, drifting instrumented buoys, and ships of opportunity. In addition, during the last 40 years, remotely sensed data from satellites have offered almost synoptic information describing the Earth's surface. This information includes sea surface temperature, which has been routinely monitored; by contrast, ocean surface salinity was not remotely measured until very recently. The Soil Moisture and Ocean Salinity (SMOS) satellite, launched in November 2009, has been the first attempt to obtain remotely sensed surface salinity data. In this context, the Barcelona World Race has provided new opportunities not only to obtain a worldwide sequence of sea surface temperature and salinity data, through one of the participating ships, but also to validate the first salinity data obtained by the SMOS.

**Keywords:** sea surface temperature and salinity · ocean circumnavigation · ocean races · ships of opportunity · SMOS

**Resum.** Els oceans no solament cobreixen aproximadament tres quartes parts de la superfície de la Terra, sinó que constitueixen el controlador més rellevant del clima. Així i tot, el coneixement que es té actualment dels oceans no es pot comparar amb el que es té dels sistemes terrestres o atmosfèrics. La salinitat i la temperatura són factors clau per entendre la dinàmica dels oceans, però encara no existeix una xarxa global d'observacions. Així i tot, s'estan obtenint dades molt valuoses dels oceans mitjançant campanyes oceanogràfiques i l'ús de dispositius automatitzats, ancoratges o boies a la deriva instrumentades i vaixells d'oportunitat. A més, durant els darrers quaranta anys, les dades obtingudes per teledetecció per satèl·lits han ofert informació gairebé sinòptica sobre la superfície de la Terra, que inclou la temperatura de la superfície del mar, monitoritzada de manera rutinària. En canvi, la salinitat superficial de l'oceà no s'ha pogut obtenir remotament fins fa molt poc. El satèl·lit SMOS (per les sigles en anglès de «humitat del sòl i salinitat oceànica»), llançat el novembre del 2009, n'ha estat el primer intent satisfactori. En aquest context, la *Barcelona World Race* ha ofert noves oportunitats per obtenir una seqüència de temperatura i salinitat superficials a escala global, a través d'un dels vaixells participants, així com per validar les primeres dades sobre salinitat obtingudes amb l'SMOS.

**Paraules clau:** temperatura i salinitat de la superfície marina · circumnavegació oceànica · regates oceàniques · vaixells d'observació d'oportunitat · SMOS

## The Earth, a planet of (salty) water

MORE THAN TWO-THIRDS OF THE EARTH'S surface is covered by salt water. The thin layer (compared to the radius of the Earth) of water that we call oceans is in continuous movement because of the action of tides, mechanical forcing provided by winds, and the potential energy created by the density contrasts between different water masses. The density of a water parcel is function of its temperature, its content of dissolved substances (summarized by a single quantity called salinity), and pressure. Accordingly, ocean density is affected by air—sea heat and mass exchange fluxes, river outflows, the freezing and melting of sea ice, mixing, and diffusion. Together, this set of processes, which are not easily observable or quantifiable, are collectively known as thermohaline forcings. At oceanic scale, water density increases with depth so that the water column appears to be stably stratified, because the oceans are heated from above and water is almost incompressible. Because of their stratification, oceans move almost horizontally, with different spatial and temporal scales at different layers. The oceanic circulation in the upper 1000 m is well known and has a characteristic time scale of months to years. Deep oceans, by contrast, were previously considered as being almost at rest. Their dynamics remained unobserved for a long time because their characteristic time scales ranged from decades to hundreds of years.

Surface ocean circulation is mainly wind-driven. Wind causes movement directly by tangential stresses that transfer momentum and indirectly by building pressure gradients. The resulting movements are predominantly horizontal but since they are constrained by the contours of land masses (bottom topography and coasts), vertical displacements occur at local and regional scales (e.g., sills, straits, coastal upwelling). Heat and mass exchanges taking place at the surface are the primary drivers of deep circulation. While the heat gain by the ocean reinforces stratification, heat losses induce water sinking and convective motions. Deep convection at regions such as the Gulf of Lions, the Labrador Sea, and the Weddell Sea play a role at basin or global scales [22]. Density changes, however, do not necessarily follow only temperature changes as ocean density also depends on salinity. At the surface, salinity changes are caused by evaporation and precipitation. Evaporation is associated with latent heat losses that decrease surface temperature in addition to the salinity increase, enhancing convection. Precipitation (as well as ice melting and riverine runoff) decreases surface salinity, thus reinforcing stratification. An example of the impact of salinity is the fact that deep water forms in the North Atlantic but not in the North Pacific, because the waters of the latter are fresher. On the other hand, negative sea surface salinity (SSS) anomalies in the North

Atlantic Ocean because of ice melting may disrupt the process of deep water formation [11]. Because of salinity, the water column in the ocean can and actually does present temperature inversions. If the surface waters receive fresh waters, they can be cooled without sinking, as is the case in freshwater bodies. Strong surface evaporation can force relatively warm surface waters to sink, with their replacement by colder and fresher waters from the sides. Both situations produce "hidden" heat storage in deep oceans, with the best examples being the two intermediate layers found in the Atlantic between 1000 and 1500 m, the Antarctic Intermediate and Mediterranean water masses.

Despite the advances achieved in physical oceanography since the end of World War II, the dynamics of the ocean are far from being completely understood or even monitored. There are two main reasons for the deficiency in our knowledge: (1) the ocean is not a linear system, so it is not possible to separate thermohaline from wind-driven circulation [10]. (2) Ocean observations are lacking, particularly before the onset of the satellite era (1980s). Furthermore, analytical, exact solutions were found for simplified (and linear) versions of the equations describing ocean dynamics. While these solutions provided qualitative descriptions of large-scale ocean circulation, they failed to reproduce the measured transports of heat and mass. With the use of numerical simulations, which provide approximations of the non-linear ocean circulation equations, our understanding of the physical processes, and of the role played by ocean transports, has improved [4,5]. However, further improvements in our ability to describe ocean dynamics require a better ocean observation system, either with a larger number of monitored variables or with increased spatial or temporal sampling rates. As emphasized below, one of the key ocean variables that still lacks a synoptic, global observational system, is salinity.

## Salinity and climate

The importance of the ocean on climate is a function of a variety of processes, ranging from its large heat storage capacity to its ability to transport heat from low to high latitudes, and from there to intermediate or deep ocean layers. For example, the top few meters of the seas store more heat energy than the entire atmosphere, and the heat absorbed by the oceans in the tropics is transported towards the poles via warm ocean currents, such as the Gulf Stream, whose heat transport is estimated to be about 1.3 petawatts ($10^{15}$ W) [16].

Salinity impacts the Earth's climate in several ways. One of them, related to its role in large-scale ocean circulation, is the above-mentioned contribution to "hidden" heat storage. Another important aspect is related to the hydrological cycle (i.e., the idealized description of the continuous movement

of water through its different phases of ice, atmospheric vapor, surface freshwaters, and the oceans). Yet, although it is one of the key climatic drivers, it remains poorly observed. For instance, evaporation (E) and precipitation and river runoff (P) are for the most part not being measured anywhere in the ocean. Salinity observations, in this context, could be used as an indicator of E-P. Moreover, salinity changes by themselves may modulate the intensity of the hydrological cycle, through the above-mentioned impacts on ocean density, the modulation of ocean convection, and the shielding provided by the barrier layer, as described below.

One of the major sources of interannual climate variability is the El Niño/Southern Oscillation (ENSO). Since pioneering, intermediate coupled ocean-atmosphere models used to predict ENSO did not account for salinity. The situation changed by the end of the 1990s, when the role of salinity in ocean dynamics was investigated [1,12,17,19] and the importance of SSS information in the prediction of ENSO was highlighted [6]. Specifically, it was shown that although SSS observations played only a small part in the statistical nowcasts of ENSO, they provided significant information in 6- to 12-month predictions. With these lag times, positive anomalies of SSS off the equator have the potential to modify the subsurface stratification of the western Pacific as they are subducted westward. In this region, the most prominent feature related to salinity is the existence of a barrier layer [15] that isolates the surface mixed layer from the entrainment of cold water from below. Thus, salinity stratification helps to preserve a warm anomaly at the surface and increases the fetch of westerly winds, facilitating the ocean-atmosphere-coupled instabilities associated with El Niño events [18]. At the eastern Pacific, the other edge of the warm pool is distinguished by a sharp SSS gradient but by a weak sea surface temperature (SST) gradient. Remote sensing of SSS is thus expected to result in an improved characterization of the state of the equatorial Pacific prior to and during the initial phases of ENSO events.

Finally, in addition to aspects related to heat storage and transport, long-term climate trends also assume a significant uptake by the ocean of atmospheric carbon dioxide ($CO_2$). Beginning with the speculations of Arrhenius, that changes in the atmospheric $CO_2$ concentration significantly modified SST [3], to the unfortunate evidence nowadays, oceans have been recognized as playing a key role in the evolution of anthropogenic $CO_2$ [20]. According to recent estimates, over the last 250 years the oceans have removed about 45 % of anthropogenic $CO_2$ [21].

In 2003, the *Second Adequacy Report* [9], compiled by the Global Climate Observing System (GCOS), formalized scientific requests for systematic climate observations to meet the needs of, among others, the Intergovernmental Panel on Climate Change (IPCC). Climate observations are needed to: (a) characterize the state of the global climate system and its variability; (b) monitor its forcings, both natural and anthropogenic; (c) help to identify the causes of climate change; (d) support climate prediction efforts; (e) infer regional and national impacts of global climate change; and (f) assess the impact of climate change on extreme events. The report defined an ensemble of essential climate variables (ECV) of the global climate system whose observation is feasible. The information provided by the ECV significantly contributes to the needs of the United Nations Framework Convention on Climate Change (UNFCCC) and the IPCC. Among the oceanic variables, temperature and salinity vertical distribution, together with their surface values were included in the ECV ensemble.

## In situ measurements of temperature and salinity

Temperature and salinity measurements have been recorded for more than a century. However, since the 1970s, improvements in battery capacity, microprocessors, and electronic recording devices, together with the advent of satellites, have led to quantitative and qualitative changes in the overall observations of the oceans. Today, satellites provide the bulk of ocean-surface information while in situ automatic sensor networks (moored or drifting) contribute the necessary complementary information (for calibration, validation, and detection of sub-surface long-term trends) on the ocean ground state.

The SST was one of the first oceanic variables to be measured, and it continues to be one of the most widely observed. Before the satellite era, most of the SST measures were obtained by thermometers (from buckets or suspended from a ship). The first automated observations of SST were obtained, in the 1960s, by placing a sensor at the intake port of a ship. Today, automatic in situ measurements are generated by buoys, floats, research ships, and ships of opportunity.

In their attempts to measure temperature below the surface (by simply sinking and retrieving mercury thermometers), scientists rapidly realized: (1) that the housings had to be carefully designed if they were to survive the high pressures of the ocean waters and (2) that the deep temperature values were modified by the water masses crossed by the thermometer on its way to being retrieved. The min-max thermometer used in the *Challenger* expedition (1873–1876) was able to record the minimum and maximum temperatures encountered during descent and ascent. The reversing thermometer, introduced in 1874, was widely used until the 1970s. This thermometer had a mechanism that once it was inverted, it fixed the temperature reading until it was inverted again. Such measures were taken at discrete depths but beginning in 1930 a mechanical device, the bathythermograph (BT), was used to obtain a continuous profile of temperature

as a function of depth. The BT was based on a stylus forced in the *y* direction by the pressure acting on a membrane and in the *x* direction by the thermal expansion of a gas in a coil.

Advances in electronics led to a new method to measure temperature, by exploiting the fact that the electrical resistance of metals, and of other materials, changes with temperature. Today, all electronic thermometers are based on this principle. One of the first oceanographic instruments to exploit this property was the expendable bathythermograph (XBT), which included a thermistor (i.e., a semiconductor used as the resistive material). In the late 1960s, XBTs provided the majority of the sub-surface continuous temperature measurements in the ocean. They replaced the earlier BTs until the generalized use of the CTD (see below), beginning in the early 1980s. The theoretical accuracy of the XBT is 0.1 °C. However, its sampling depth was not measured but was instead calculated from the estimated fall rate. The various sources of uncertainty led to XBT values that were usually biased. Consequently, early estimates of global ocean climate change were distorted.

Ocean salinity has been measured since the first oceanographic campaigns, through the analysis of water samples, taken either at the surface or at any depth. The chemical composition of seawater was first reported in 1877, from data collected throughout the *Challenger* expedition. Since then, there have been no apparent changes in the composition of seawater. In addition, there have been no significant salt losses in the ocean, with salinity only changing by mixing or by the addition or removal of freshwater via precipitation or evaporation. Thus, it can be assumed that for the time scales pertinent to climate change, i.e., decadal to centennial, salinity behaves as a conservative tracer. As the salt composition is almost constant and chloride is its most important component, until the 1950s, salinity was obtained by a chemical analysis of chlorinity. Later on, since electrical conductivity of the water depends on both salinity and temperature, salinity was measured based on the conductivity of the sampled water at a fixed temperature.

The development of electronic instruments to measure conductivity and temperature evolved to yield thermosalinographs, which since the 1970s have provided continuous surface temperature and salinity data along a ship's track. A subsequent development included a pressure sensor and resulted in the conductivity-temperature-depth (CTD) probe, which is able to provide continuous vertical profiles of temperature and salinity as deep as 10,000 m and is routinely used in all oceanographic cruises. In fact, since the 1980s the CTD has been the standard tool to determine essential physical properties of the oceans. Based on CTD technology, autonomous probes have been developed during the last 20 years that can be installed in fixed moorings, in drifting buoys, and in automatic drifting profilers, called Argo profilers. These

probes have been routinely launched in all the oceans since 1997, within the framework of the international Argo program [http://www.argo.ucsd.edu], which maintains ~3000 active profilers to provide worldwide coverage. The long-term stability and accuracy of the conductivity measurements are still an issue when the CTD probes are continuously deployed (e.g., Argo profilers and moorings).

## Satellite measurements of temperature and salinity

In general, satellite measurements have the advantage of being synoptic over large areas and the disadvantage of providing information only for a thin layer of the sea surface in contact with the atmosphere. Since the SST provides the boundary condition for estimating air-sea heat fluxes, having this information on a global scale offers insights into the heat balance in the climate system, general circulation patterns, and thermal anomalies. At smaller scales, it can provide information about the presence of fronts between different water masses and the intensity of coastal and equatorial upwelling.

Satellite estimates of SST rely on thermal emissions from the surface through the atmosphere. The use of infrared (~3.7 μm and/or ~10 μm) radiometers dates back to the end of the 1960s. The main drawback of infrared observations is that they are obscured by clouds. More recently, passive microwave (4–10 GHz) measurements have resolved this problem, although their precision is lower than infrared estimates because microwave emission is not as strongly tied to the temperature of an object as infrared. Since the two methods have different strengths and weaknesses, their combination provides the most accurate SST data.

As was the case for SST measurements before they were obtained by satellites, historical SSS knowledge mostly came from single water samples, followed by thermosalinograph measurements onboard research vessels and ships of opportunity, and from moored buoys. However, the success of obtaining satellite-based SST measurements contrasts with the fact that no remotely sensed data of density or salinity were acquired until very recently, i.e., more than 40 years later.

The ability to estimate SSS from space relies on the fact that at low frequencies, including microwave, the thermal emissions of the ocean are proportional to its physical temperature. The proportionality coefficient, the emissivity, is a function of the dielectric constant, which depends on conductivity, i.e., salinity. The launch of the Soil Moisture and Ocean Salinity (SMOS) satellite by the European Space Agency in November 2009, followed some months later by the launch of Aquarius by the National Aeronautics and Space Administration (NASA), finally opened the door to the remote monitoring of SSS. Both instruments exploit the

fact that significant information on sea surface dielectric properties (related to salinity) can be retrieved from ocean microwave emissions, particularly L-band (1.40–1.43 GHz), at which the sensitivity of surface emissivity to salinity is the largest. The SMOS and the Aquarius-SAC/D mission are the first two space missions designed to provide global, synoptic estimates of the SSS, with an accuracy of about 0.1 psu (practical salinity units) every 30 days and a spatial resolution of 200 km.

The weak sensitivity of brightness temperatures to salinity hinders the retrieval of the latter, with averaging over 10–30 days required to reduce random errors. In fact, after processing of the first 18 months of SMOS data, it has become clear [8] that the narrow range in brightness temperatures of ocean emissions, the unexpectedly large amplitude of the errors associated with the image reconstruction process, and the complex forward geophysical modeling (relating the physical parameters of the sea surface with the microwave emissions detected by satellite) make the retrieval of salinity from SMOS data very challenging. It is therefore critical to use in situ data to calibrate and validate remotely sensed SSS.

## New opportunities. The Barcelona World Race survey

Gathering temperature, salinity, and as other relevant measures needed to understand the behavior of the ocean requires immense efforts: equipping ships, deploying instruments and satellites, transmitting information, etc. A limited number of oceanographic campaigns, fixed moorings, drifting buoys, automatic profilers, etc. cover a wide area of the ocean but the spatial and time distribution of this coverage is very irregular. Indeed, at any given time, several large regions are completely uncovered while others are heavily sampled. Moreover, the actual distribution of sampling changes continuously, according to the interests of the various oceanographic studies. Most of them are local or regional in scope while others cover large regions. Further complications are that similar oceanic sections are scarce, some sections are unique, and large regions of the oceans have never been sampled. There is also no worldwide network that collects oceanographic data, as is the case for meteorological stations, although climatic and even meteorological models would benefit immensely from oceanic information.

In addition to automated methods such as drifting buoys and Argo profilers, ships of opportunity can provide complementary oceanographic information. During the last 20 years, an increasing number of ferries and carriers have been equipped with thermosalinographs that report surface data along the vessels' tracks. Although the data obtained are very useful at large scale, they are restricted to commercial routes and, again, most of the oceans, especially the



**Fig. 1.** *The Fòrum Marítim Català* (*FMC*), an Open 60 sailing boat that participated in the second edition of the Barcelona World Race. The *FMC* was equipped with an ocean temperature and salinity sensor and a transmitter able to provide real-time data along its around-the-world ocean trip from December 2010 to April 2011. (Image courtesy of *FMC*).
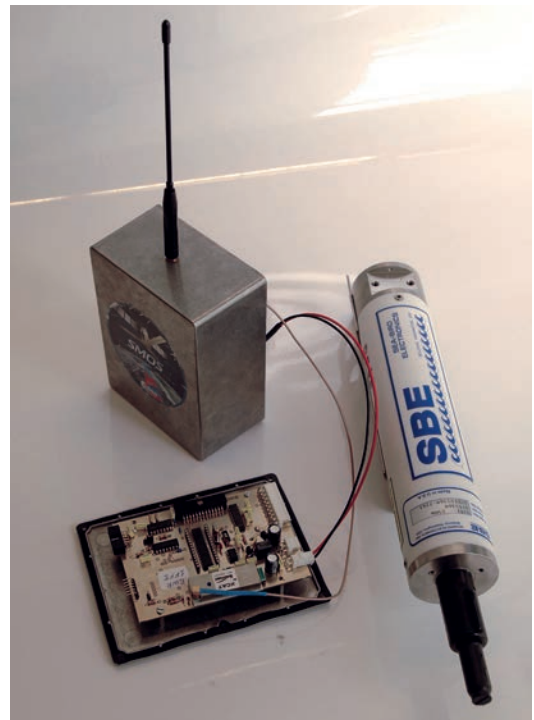


**Fig. 2.** Detail of the Sea-Bird SeaCat temperature and salinity sensor and the transmitter that were installed onboard the *FMC*.

southern ones, remain uncovered. Progress in this regard started in 2010, when the organizers of the Barcelona World Race (BWR) together with scientists from the Institute of Marine Sciences (ICM-CSIC), and members of the Maritime Catalan Forum (FMC) agreed to equip the *FMC* boat (Fig. 1) participating in the BWR with a MicroCAT temperature and conductivity sensor and an XCAT transmitter (Fig. 2). The idea was to find out whether oceanic races could be exploited to monitor surface temperature and salinity in the world's oceans in real time but without interfering with navigation or penalizing the boats competitiveness in the race.

The BWR is a non-stop regatta around the world, starting and ending in Barcelona every three years. Its second edition began in December 2010. The *FMC* boat completed the round trip (more than 51,000 km) in 112 days, sending 12–30 real-time temperature and salinity measures/day via
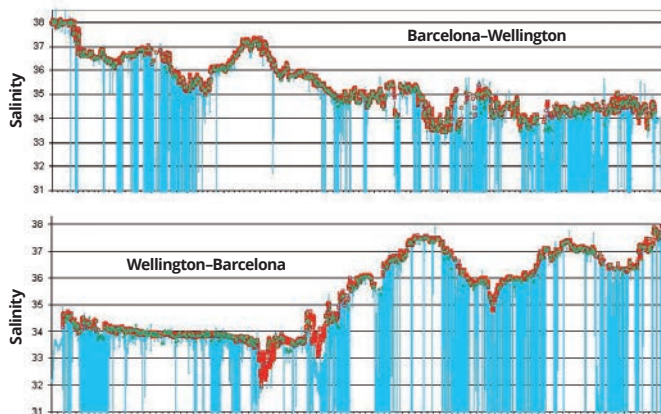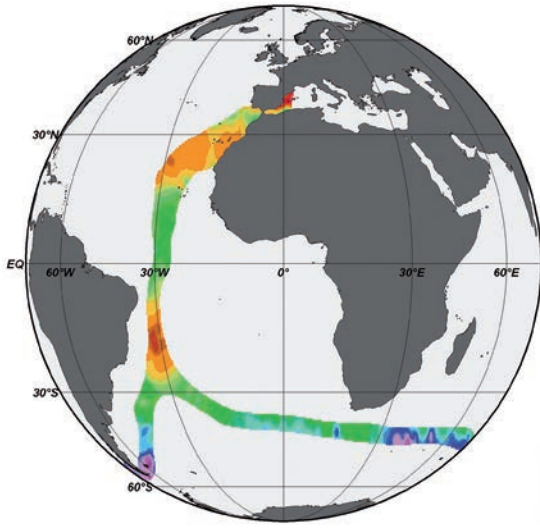
Argos satellites, using a data protocol developed at the ICM. The measuring instrument was located on the bottom of the boat, in the box housing the articulation of the swing keel (Fig. 3). Although this box was open and below the waterline, ensuring good renewal of the water, it was exposed to bubbles in rough weather and even dry in case of high inclination, especially when the boat sailed against the wind. The data were stored in an internal memory at a rate of 8 scans per hour and transmitted via Argos satellites every 90 s. This gave a redundancy of six repeated measurements, in order to minimize error transmission. Instantaneous positions were estimated by the Argos constellation with low precision but were adjusted later according to the official race tracking. After a first estimation of errors, preliminary data were available with a delay of 2–3 days. At the end of the race, the instrument was recovered and the data stored in the internal memory were used in a second correction and to cover gaps in transmission. A final sequence of almost 10,000 samples of SST and SSS was obtained, with a mean spatial resolution of 5 km along the track, a maximum gap of 450 km, and 16 gaps of more than 80 km without any reliable data (Fig. 4).

## Examples of direct results

The current BWR survey of SST and SSS is the longest record of this nature ever obtained. For the first time, continuous surface monitoring has been performed during a round trip around the world's oceans and in less than 4 months. The survey includes two passages over the Atlantic ocean, around two months apart (Fig. 5) and a complete circumnavigation of the Southern Ocean at latitudes between 30° and 56° S in less than 2 months (Fig. 6), covering wide regions rarely sampled. As shown in figures 5 and 6, the relatively high sampling frequency allowed for mesoscale resolution, revealing the position of the main oceanic fronts and thus a comparison of zones of high and low mesoscale activity, identification of the surface signature of the main oceanic water masses, and even an estimate of the impact of seasonal continental ice melting near Cape Horn.

The temperature-salinity (TS) diagram in Figure 7 shows the two mode waters of the Atlantic Ocean. The North Atlantic central water (NACW) and the South Atlantic central water (SACW) are clearly separated and each has very stable properties, as shown by the overlapping of the two transits, from N to S in January 2011 and from S to N two months later. Of particular interest is the good overlap between the eastern and western SACW, separated by more than 5000 km at 40°S. Two transition zones are also clearly depicted in the TS diagram. In the northern hemisphere, there is a diapycnal transition, along the track between the Cape Verde islands and Brazil, between western equatorial



**transmitter and antenna**

**MicroCAT sensor**

The swing keel is operated by very powerful hydraulic rams which press of the head of the keel. The fulcrum or keel hinge is at hull level with just a short stub on which the rams press.

**Fig. 3.** Sketch of the installation of the sensor and transmitter onboard the *FMC*.



**Fig. 4.** Time series of surface salinity data obtained by the *FMC* along its track: (a) Barcelona–Wellington through the Atlantic (N to S) and Indian Oceans, and (b) Wellington–Barcelona, through the Pacific and Atlantic (S to N) oceans. Raw data in blue, transmitted data in green, and finally accepted data in red.

*Sal [ppt] @ Depth [m]=Top*

*Sal [ppt] @ Depth [m]=Top*

**Fig. 5.** Sea surface salinity obtained by the *FMC* during the Barcelona World Race along two transits through the Atlantic Ocean. Data are extrapolated into a band ~100 km wide across the track.
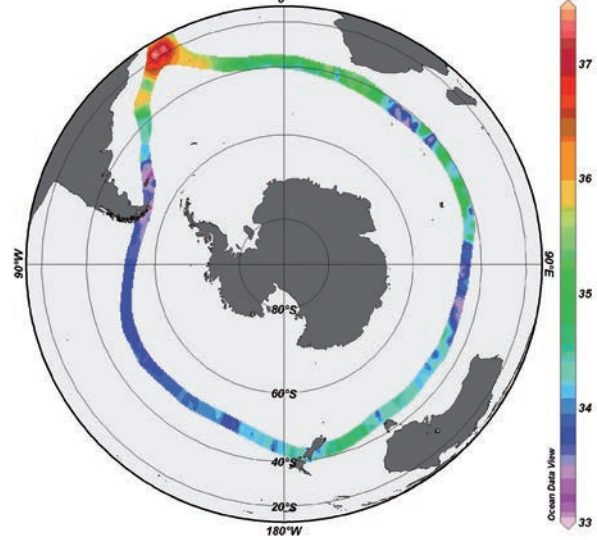
**Fig. 6.** Sea surface salinity obtained by the *FMC* during its participation in the Barcelona World Race along a transit through the Southern Indian and Pacific Oceans. Data are extrapolated into a band ~100 km wide across the track.

*Temp [deg.C]*
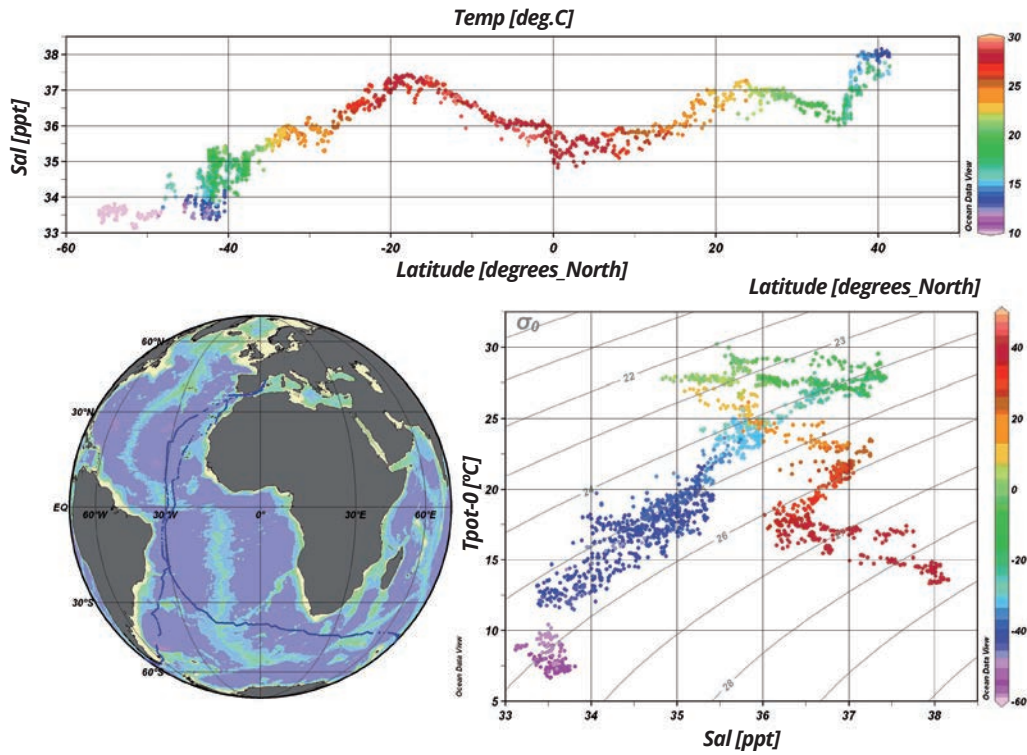
**Fig. 7.** *FMC* data obtained during its participation in the Barcelona World Race along two transits through the Atlantic Ocean, shown below on the left side of the map. Upper panel: salinity and temperature (color scale) vs. latitude. Lower panel, right: temperature-salinity (TS) diagram, with latitude presented in color scale.

waters, under the influence of riverine inputs and heavy precipitation, and the eastern NACW, which is saltier and slightly colder. In the southern hemisphere, the transition between the SACW and the equatorial waters occurs along the Brazilian coast at almost constant temperature. This difference in temperature among the equatorial transitions in the northern and southern hemispheres can be ascribed to the respective season, winter and summer, at the time of the survey. Finally, the diagrams of Figure 7 also show the Mediterranean water masses and the transition to the NACW. In this case there are slight but significant differences between the outgoing and ongoing tracks, because of the time lapse of almost 4 months between January and April 2011, that is, early winter and early spring.

The water masses along the circumnavigation from the Cape of Good Hope to Cape Horn, covering the Southern Indian and Pacific Oceans, are less definite, especially along the Indian Ocean (Fig. 8), where mesoscale activity is high because of the weather conditions and the fact that the track roughly followed the sub-tropical front, with several crossing points. The situation is clearer in the Pacific Ocean (Fig. 9), where the SASW dominates the water mass structure at the surface between the two main fronts, the sub-

tropical and the sub-Antarctic. The TS diagram also clearly depicts the coastal influence across the Cook Straits under the coastal waters of the western South Pacific, and along Cape Horn, under the effect of Patagonian ice melting.

Figure 10 shows the passage along Cape Horn in detail. Temperature, salinity, and density were spatially interpolated using the DIVA method [23] over a 100 km wide band. This interpolation allows the impact of ice melting on these variables, and especially on salinity, to be visualized, although there is not enough information to estimate freshwater flow. Only a very rough estimate is possible, since the only observed data are the mean salinities and the wideness of the patch can be reasonably estimated, whereas direct information on current velocity and patch thickness are lacking. Based on an estimated patch width of ~50 km, a mean salinity of ~32.5, and an incoming salinity of ~34, and assuming a mean thickness of 10–20 m and a mean incoming current of ~0.2 m/s, the resulting freshwater flow would be between 5000 and 10,000 $m^3$/s. But since this result is only based on the observed salinity and horizontal dimensions of the patch, its use is limited to an indicator of the order of magnitude of the melting process at the end of the austral summer.
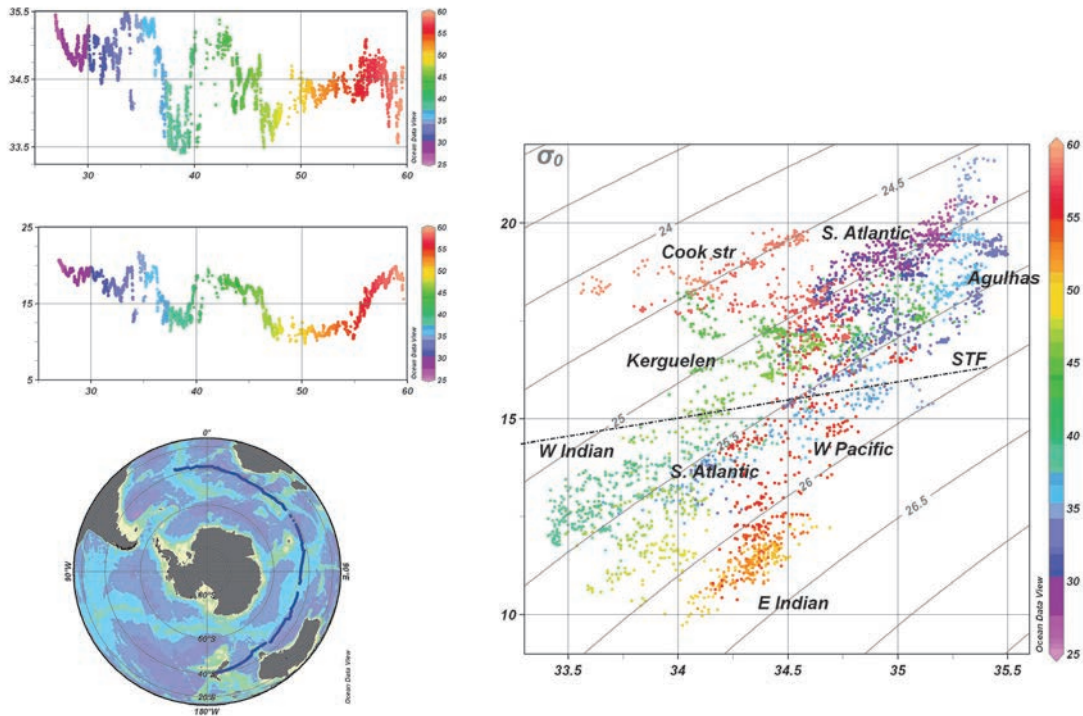


**Fig. 8.** Data obtained along the Southern Indian Ocean by the *FMC* during its participation in the Barcelona World Race, shown below on the left side of the map. Upper left panels: salinity and temperature vs. time (days from the race start). Right panel: TS diagram, with time shown in a color scale. The TS characteristics of the sub-tropical front are also shown.
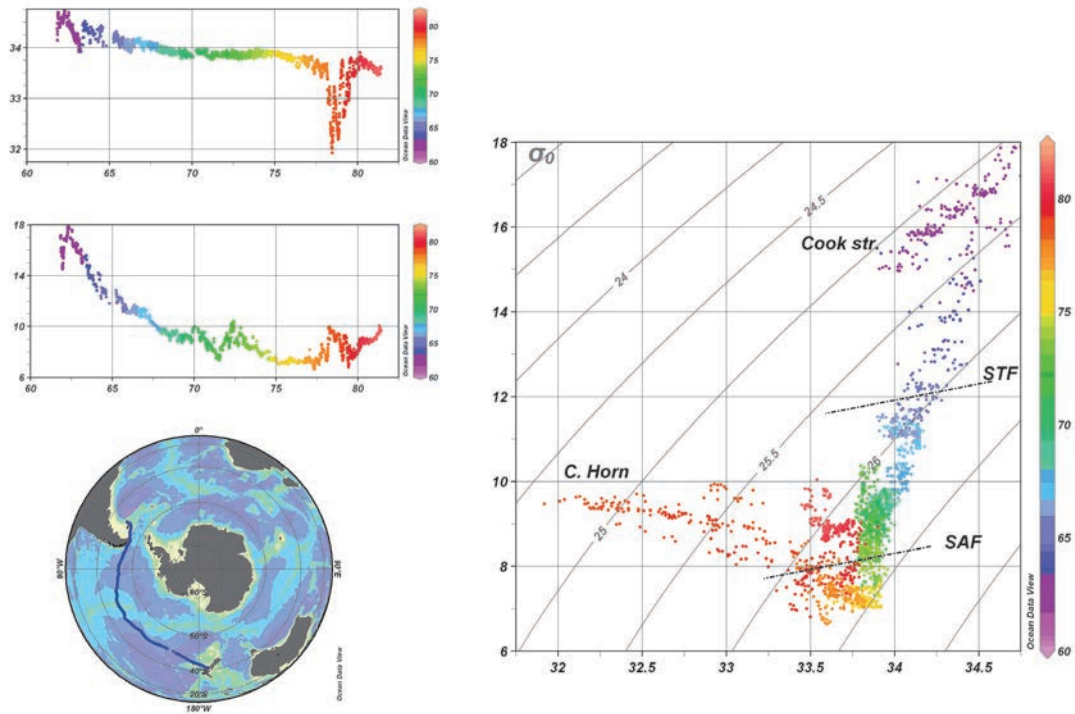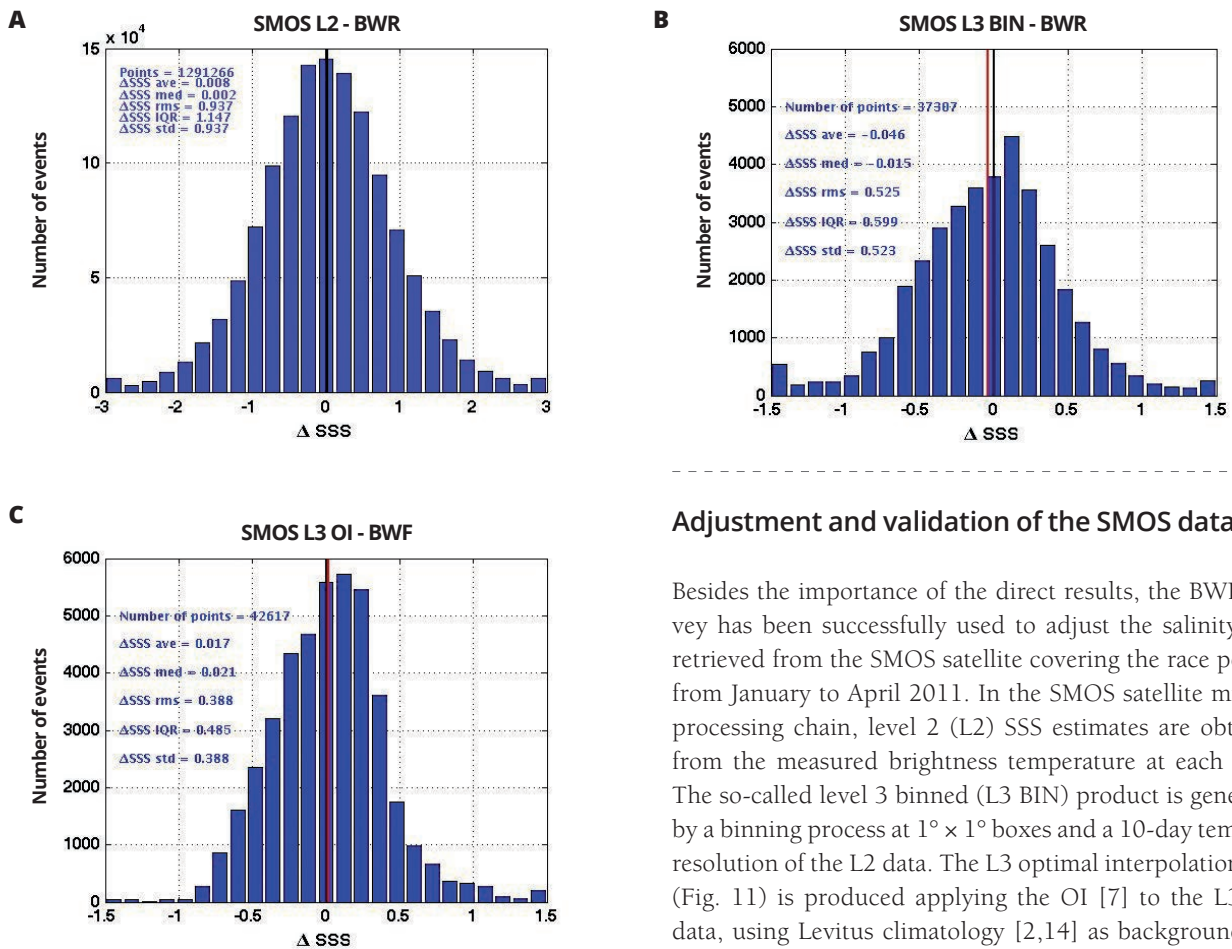
**Fig. 9.** Data obtained along the Southern Pacific Ocean by the *FMC* during its participation in the BWR, shown below on the left side of the map. Upper left panels: salinity and temperature vs. time (days from the raced start). Right panel: TS diagram, with time shown in a color scale. The TS characteristics of the sub-tropical and sub-Antarctic fronts are also shown.

-----
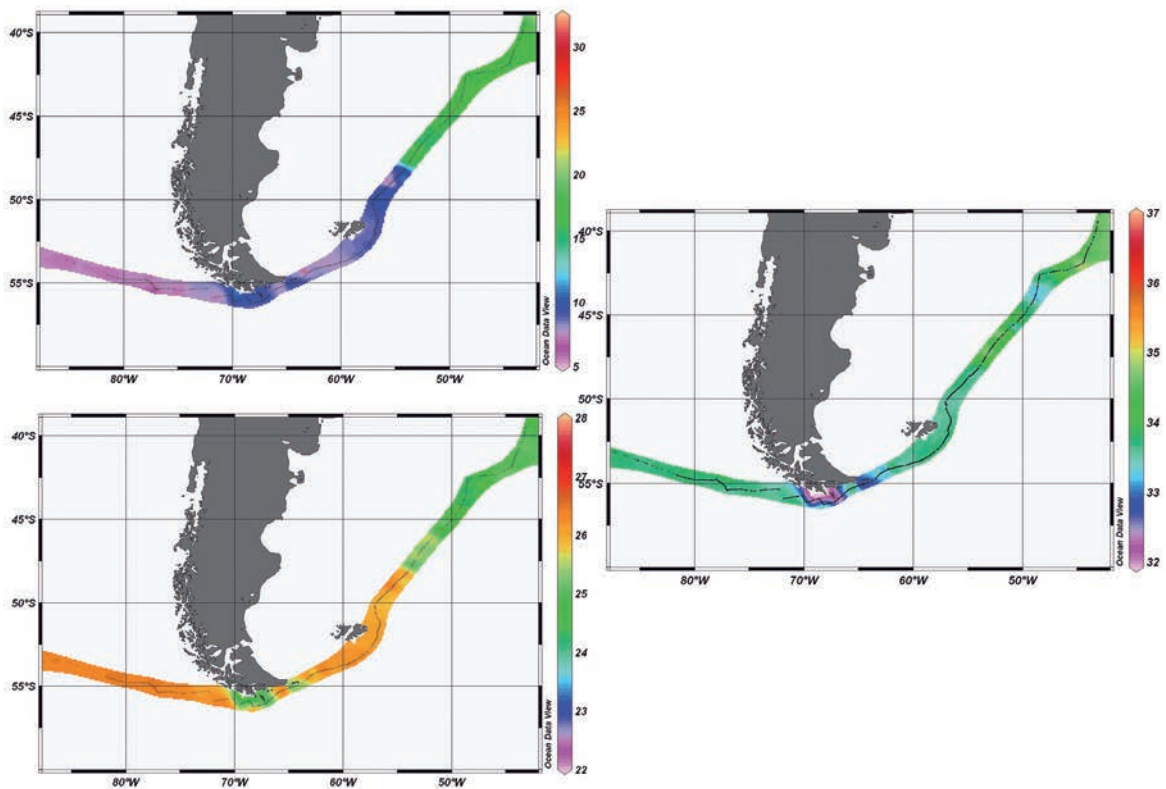


**Fig. 10.** *FMC* data obtained across Cape Horn. Left upper panel, temperature. Left lower panel, density ($\sigma_t$). Right panel, salinity. Data are extrapolated into a band ~ 100 km wide across the track.
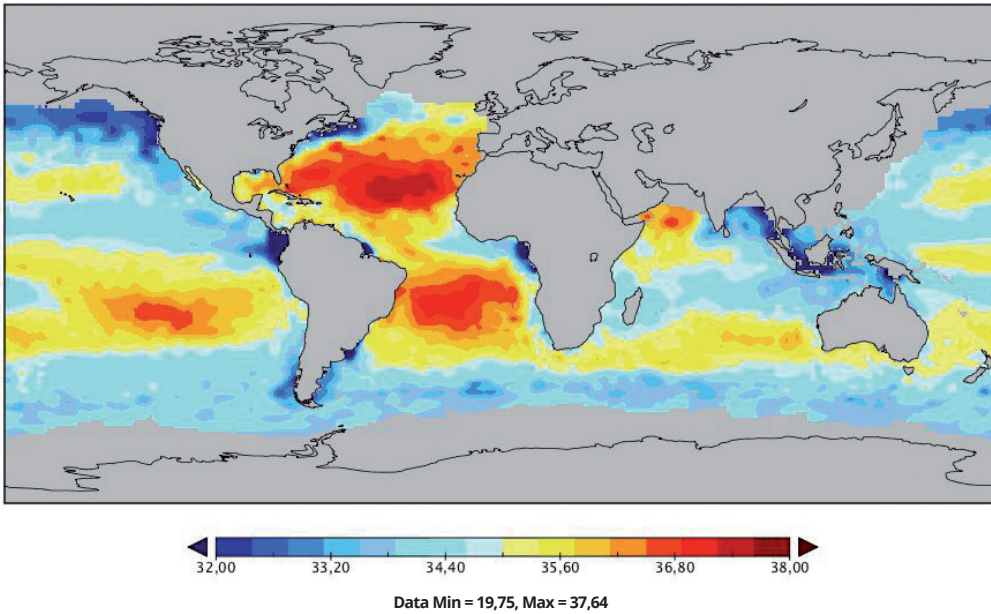
**Fig. 11.** Sea surface salinity (SSS) on January 11, 2011. The map was generated with the optimal interpolation algorithm and using 48 h of level 2 SSS data gridded onto a 1° cell.





## Adjustment and validation of the SMOS data

Besides the importance of the direct results, the BWR survey has been successfully used to adjust the salinity data retrieved from the SMOS satellite covering the race period, from January to April 2011. In the SMOS satellite mission processing chain, level 2 (L2) SSS estimates are obtained from the measured brightness temperature at each pixel. The so-called level 3 binned (L3 BIN) product is generated by a binning process at 1° × 1° boxes and a 10-day temporal resolution of the L2 data. The L3 optimal interpolation (OI) (Fig. 11) is produced applying the OI [7] to the L3 BIN data, using Levitus climatology [2,14] as background and the following background error covariance:

**Fig. 12.** Histograms of the differences between the sea surface salinity estimated by SMOS at different levels: (**A**) L2, (**B**) L3 BIN, and (**C**) L3 optimal interpolation, and data provided by the *FMC*.

$$F(\Delta x, \Delta y) = F_0 e^{-\mathbf{A}\Delta x^2 - \mathbf{B}\Delta y^2 - \mathbf{C}\Delta x\,\Delta y}$$

98

where A, B, and C are the reciprocals of the squared correlation lengths as described in [13]. The map (Fig. 11) reproduces the main features of the SSS distribution, although the filtering properties of the OI algorithm have reduced most of the mesoscale signatures of salinity.

A comparison of the results shown in Figure 11 with the SSS data recorded by the *FMC* boat along its race trajectory (Figs. 5 and 6) clearly shows that the boat's high-frequency sampling provides information on the mesoscale variability
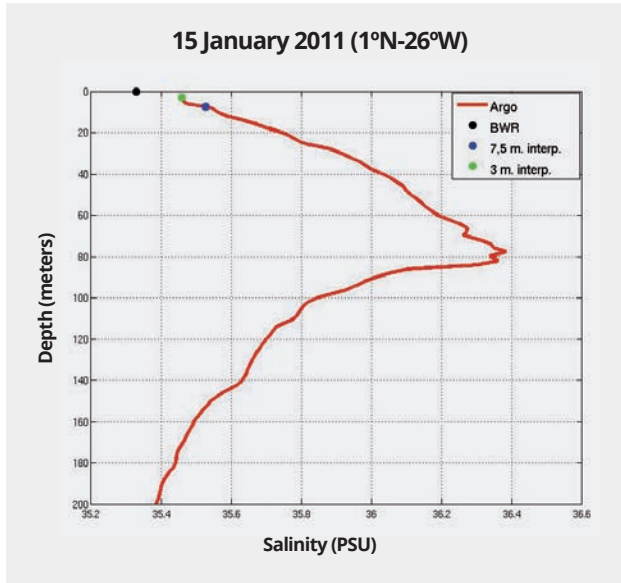


**Fig. 13.** A vertical profile of salinity, at 1°N 26°W for January 15, 2011, as determined by an Argo profiler (red), the interpolated salinity at 7.5 m (blue) and 3 m (green), and the surface salinity value recorded by the *FMC* during the Barcelona World Race (black).

of the ocean that is not resolved by the SMOS binned maps with the decorrelation lengths used in the above equation. One of the interesting features emerging from this plot is the high degree of variability in the Southern Ocean, mostly linked to the frontal regions, especially the sub-tropical front (see above).

The histogram of the difference between the SSS estimated by SMOS at the L2 level and the data provided by the BWR, corresponding to the entire race period, is shown in Figure 12a. The standard deviation of the differences is larger than 0.94 and the average difference is about 0.01. Figures 12b, and 12c show, respectively, the histograms of the differences between the BWR and the L3BIN and the L3OI, respectively. The most interesting feature of these results is the progressive noise reduction in the SSS data as higher level salinity products are introduced: the standard deviation shifts from the above mentioned 0.94 for L2 to 0.52 for L3BIN and 0.39 for L3OI.

The continuous presence of ~3000 Argo profilers scattered worldwide are being routinely used to validate the SMOS data (http://tarod.cmima.csic.es/). In this case, the information on SSS has to be extrapolated since the upper salinity value obtained by any profiler is at 7.5 m. Figure 13 provides a comparison between the information provided by an Argo profiler on 15 January 2011 at 1°N 26°W and the *FMC* surface value at the same time and place. The SSS value is lower than the extrapolated values obtained by the profiler at 3 and 7.5 m.

On a global scale, there are also differences between the optimally interpolated maps obtained from Argo profilers at 7.5 m depth and the BWR data (Fig. 14). The mean difference of 0.2, with the BWR data being more recent, could
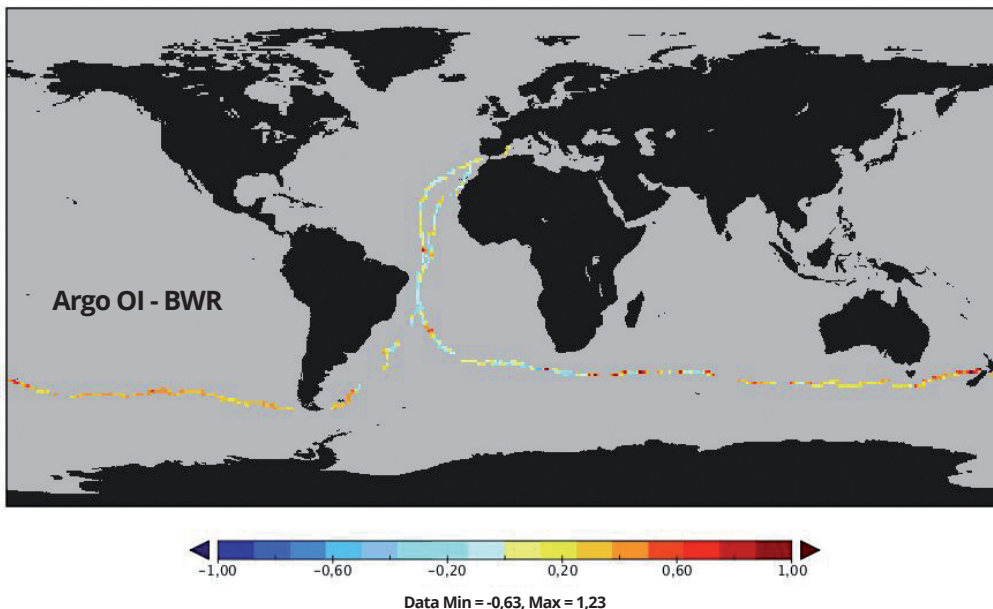


**Fig. 14.** Differences between the optimally interpolated salinity from the Argo profilers and the data recorded by *FMC* along the trajectory of the Barcelona World Race.

reflect the existence of uppermost salinity gradients not detected by the Argo profilers. Again, larger anomalies can be found in the Southern Ocean, where there are remarkable SSS fronts, because BWR data resolve mesoscale features and Argo OI fields do not.

## New perspectives and conclusions

The information on SST and salinity obtained through the participation of the *FMC* in the BWR has contributed to the study of the ocean's properties on a global scale, especially because the vessel's route covered rarely sampled regions in the Southern Ocean.

In particular, SSS data from the BWR has been successfully used to validate SMOS products, at least as well as the Argo profilers, providing a high-resolution view of the SSS along the path of the boat. The success of the present experience recommends incorporating similar temperature and salinity sensors on all the participating boats in the new editions of the BWR. This perspective will substantially increase the utility and performance of the information. On the one hand, redundancies will help to improve the data quality and, on the other, comparisons between data that are close in time and space will make available more information about the characteristics of mesoscale activities. This is especially relevant for large areas of the Southern Ocean, where until now there have been few mesoscale studies based on in situ data. ◺

## References

1.  Acero-Schertzer CE, Hansen DV (1997) Evaluation and diagnosis of surface currents in the National Centers for Environmental Prediction's ocean analyses. J Geophys Res 102:21037-21048
2.  Antonov JI, Seidov D, Boyer TP, Locarnini RA, Mishonov AV, Garcia HE, Baranova OK, Zweng MM, Johnson DR (2010) World Ocean Atlas 2009, Vol. 2. In: Levitus S (ed) Salinity. Ed NOAA Atlas NESDIS 69, U.S. Government Printing Office, Washington DC
3.  Arrhenius S (1896) On the influence of carbonic acid in the air upon the temperature of the ground, Phil Mag 41:237-76
4.  Anderson DLT, Stockdale T, Balmaseda M, Ferranti L, Vitart F, Molteni F, Doblas-Reyes F, Mogensen K, Vidard A (2006) Development of the ECMWF seasonal forecast system 3. ECMWF Technical Memorandum 503
5.  Bahurel P, Mercator Project Team (1999) Mercator, developing an integrated system for operational oceanography. In: OceanObs99 Proceedings, The Ocean Observations Conference, Saint Raphael 17th to 22 October 1999 [http://www.oceanobs09.net/work/oo99/docs/Bahurel.pdf]
6.  Ballabrera-Poy J, Murtugudde R, Busalacchi AJ (2002) On the potential impact of sea surface salinity observations on ENSO predictions. J Geophys Res 107:C12, 8007. doi:10.1029/2001JC000834
7.  Bretherton FP, Davis RE, Fandry CB (1976) A technique for objective analysis and design of oceanographic experiments applied to MODE-73. Deep-Sea Res 23:559-582
8.  Font J, Camps A, Borges A, Martín-Neira M, Boutin J, Reul N, Kerr Y, Hahne A, Mecklenburg S (2010) SMOS: The challenging measurement of sea surface salinity from space. Proc IEEE, 98:649-665
9.  GCOS (2003) The second report on the adequacy of the global observing systems for climate in support of the UNFCCC. GCOS-82 (WMO/TD No. 1143), World Meteorological Organization, Geneva
10. Gill AE (1982) Atmosphere-ocean dynamics. Academic Press, New York
11. Häkkinen S (1999) A simulation of thermohaline effects of a Great Salinity Anomaly. J Clim 12:1781-1795
12. Ji M, Reynolds RW, Behringer DW (2000) Use of TOPEX/Poseidon sea level data for ocean analyses and ENSO prediction: some early results. J Clim 13:216- 231
13. Jordà G, Gomis D, Talone M (2011) The SMOS L3 mapping algorithm for sea surface salinity. IEEE Trans Geosci Remote Sens 49:1032-1051
14. Levitus S, Boyer TP, Conkright ME, O'Brien T, Antonov J, Stephens C, Stathoplos L, Johnson D, Gelfeld R (1998) NOAA Atlas NESDIS 18, World Ocean Database 1998, Vol 1, Introduction. U.S. Gov. Printing Office, Washington DC
15. Lukas R, Lindstrom E (1991) The mixed layer of the western equatorial Pacific. J Geophys Res 96:3343-3357
16. Lund DC, Lynch-Stieglitz J, Curry WB (2006) Gulf Stream density structure and transport during the past millennium. Nature 444:601-604
17. Maes C (2000) Salinity variability in the equatorial Pacific Ocean during the 1993–98 period. Geophys Res Lett 27:1659-1662
18. Maes C, Picaut J, Belamari S (2002) Salinity barrier layer and onset of El Niño in a Pacific coupled model. Geophys Res Lett 29:2206. doi:10.1029/2002GL016029
19. Murtugudde R, Busalacchi AJ (1998) Salinity effects in a tropical ocean model, J Geophys Res 103:3283-3300
20. Revelle R, Suess H (1957) Carbon dioxide exchange between atmosphere and ocean and the question of an increase of atmospheric $CO_2$ during the past decades. Tellus 9:18-27
21. Sabine CL, Feely RA, Gruber N, Key RM, Lee K, Bullister JL, Wanninkhof R, Wong CS, Wallace DWR, Tilbrook B, Millero FJ, Peng T-H, Kozyr A, Ono T, Rios AF (2004) The oceanic sink for anthropogenic $CO_2$. Science 305:367-371
22. Straneo F (2006) On the connection between dense water formation, overturning, and poleward heat transport in a convective basin. J Phys Oce 36:1822-1840
23. Troupin C, et al. (2012) Generation of analysis and consistent error fields using the Data Interpolating Variational Analysis (Diva). Ocean Modelling 52-53:90-101